

Supplementary Information

A honeycomb-like porous carbon derived from pomelo peel for use in high-performance supercapacitors

Qinghua Liang,^{†ab} Ling Ye,^{†ab} Zheng-Hong Huang,^{*b} Qiang Xu,^b Yu Bai,^b Feiyu Kang^{ab} and Quan-Hong Yang^{*ac}

^a Engineering Laboratory for Functionalized Carbon Materials, Graduate School at Shenzhen, Tsinghua University, Shenzhen 518055, China.

^b Key Laboratory of Advanced Materials (MOE), School of Materials Science and Engineering, Tsinghua University, Beijing 100084, China

^c School of Chemical Engineering and Technology, Tianjin University, Tianjin 300072, P. R. China

1. Experimental section

1.1 Synthesis of pomelo peel-derived HLPC

The detailed preparation procedure is illustrated in Fig.S1. In a typical process, a small piece of pomelo peel was dried at 60 °C for 12 h, and was then disintegrated in an agate mortar. The white powder was pre-carbonized at 400 °C with a heating rate of 5 °C min⁻¹ for 1 h under N₂ flow. Afterwards, the resulting black powder was further grounded and thoroughly mixed with different volume of 1 M KOH aqueous solution. Then, the black paste was dried at 80 °C for 4 h to remove redundant water, and was further grounded to ensure KOH was mixed evenly. Subsequently, the resultant mixture was placed in a nickel crucible and heated at 5 °C min⁻¹ with the protection of N₂ by the following procedure: it was first heated to 450 °C and was kept at this temperature for 30 minutes; then, the temperature was increased to 650 °C and hold for another 30 minutes; finally, the temperature was raised to 800 °C and kept for 1.0 hour. Finally, the as-obtained activated sample was washed with 1 M HCl to remove any inorganic impurities, and then washed thoroughly with distilled water until pH ≈ 7. A series of experiments were similarly carried out to

investigate the amount of KOH on the microstructure and electrochemical performance of the HLPC. The resultant HLPC was designated as S1, S2, S3, and S4 when the weight ratio of KOH and pre-carbonization product is 1: 2, 1: 1, 1.5:1, and 2:1, respectively.

1.2 Sample structure and morphology characterizations

The morphology and microstructure of the as-prepared HLPC were observed with field emission scanning electron microscopy (SEM, Hitachi S-4300) and transmission electron microscopy (TEM, JEOL-2100F) at an acceleration voltage of 200 kV. The surface functional groups were investigated by Fourier transforms infrared spectra (FT-IR, Varian Excalibur 3100). The structure was examined using Raman scattering spectra (Renishaw, InVia-Reflex) using laser excitation at 532 nm. The phases were examined by X-ray diffraction (XRD, Bruker D8-ADVANCE) operating at an acceleration voltage of 40 kV. The Nitrogen adsorption-desorption isotherms were obtained at 77 K on a Quadrasorb SI-MP Analyzer. The SSA was calculated by Brunauer–Emmett–Teller (BET) method. The pore size distribution was analyzed by the nonlocal density functional theory (DFT) method by using nitrogen adsorption data with a slit pore model. The total pore volume was estimated from the adsorbed amount at a relative pressure $P/P_0 \approx 0.995$. The elemental analysis and surface states were characterized by X-ray photoelectron spectroscopy (XPS, VG Scientific ESCA LAB 220i-XL) with an excitation source of Al K α X-ray source.

1.3 Electrochemical measurements

All the electrochemical measurements were carried out on a Bio-Logic electrochemical workstation (VMP3, France) at room temperature. Three-electrode system tests were carried out in 6.0 M KOH aqueous solutions with Pt wire as counter electrode and Hg/HgO electrode as reference electrode. The working electrode was fabricated by coating the mixture containing 85 wt% active materials, 10 wt% poly(tetrafluoroethylene) (PTFE, 60 wt% in water) and 5 wt % Super P on a 1 cm \times 2 cm nickel foam. After the electrode materials were loaded, the working electrode was dried in vacuum at 120 $^{\circ}$ C for 12 h and then pressed at 5 MPa for 5 s. The amount and effective area of active materials on each current collector was about 2 mg and 1.0 \times 1.0 cm 2 , respectively. Cyclic voltammetry (CV) curves were obtained in the potential range of $-1.0-0$ V vs Hg/HgO at various scan rates from 5.0 to 200 mV s $^{-1}$. The constant current charge–discharge

capacitance measurements was conducted on an Arbin testing system with different current densities from 0.2 to 20 A g⁻¹ with a potential window of -1.0-0 V. Electrochemical impedance spectroscopy (EIS) measurements were carried out for the working electrode in a frequency range of 200 kHz to 10 mHz at open circuit potential with an amplitude of 5 m V. The EIS data were analyzed in the form of Nyquist plots. The cyclic stability was evaluated by constant current charge/discharge measurements at a current density of 10 A g⁻¹ for over 1000 cycles. The gravimetric specific capacitance of the electrode composites based on the three-electrode system was calculated from the charge/discharge curves using the following equation:

$$C = I \times \Delta t / (m \times \Delta V)$$

Where C (F g⁻¹) represents the specific capacitance of the active material, I (A) refers to the discharge current, Δt (s) is the discharge time, ΔV (V) corresponds to the potential change within Δt , and m (g) is the mass of the active material loaded in the working electrode. The gravimetric specific capacitance (C_v) was calculated by the equation of $C_v = \rho \times C$, where ρ is the bulk density and C is the gravimetric specific capacitance.^{1,2}

The symmetric SC was conducted in a 2032 stainless steel coin cell with two nearly identical electrodes using a cellulose acetate membrane as separator, two pieces (1.0 × 1.0 cm²) of nickel foil as the current collectors, and 6 M KOH aqueous solutions as the electrolyte. The working electrodes were prepared by the same procedure as the three-electrode system except that the circular nickel foam was assembled onto stainless steel mesh under pressure. The electrochemical performance of SC was determined by the CV and galvanostatic charge/discharge. CV tests were measured at various scan rates from 5.0 to 200 mV s⁻¹. The charge/discharge measurements were performed on an Arbin testing system with a constant current from 0.2 to 20 A g⁻¹ with a potential window of 0-1.0 V. EIS tests were also carried out in a frequency range of 200 kHz to 10 mHz at open circuit potential with an amplitude of 5 m V. The cyclic stability was evaluated by constant current charge/discharge measurements at a current density of 5 A g⁻¹ for over 1000 cycles. The specific capacitance of the SC cell was calculated by using the following formula:

$$C_{cell} = I \times \Delta t / (m \times \Delta V)$$

Where C_{cell} (F g⁻¹) is the specific capacitance of the cell (based on the mass of active materials), I (A) corresponds to the discharge current, Δt (s) refers to the discharge time, ΔV (V) represents the potential change within Δt (s), and m (g) is the total mass of the active materials loaded on the two

working electrodes. The power (P) and energy density (E) were calculated based on the following equation:

$$E = 1/2 \times C_{cell} \times (\Delta V)^2$$

Where E ($J g^{-1}$) represents the energy density, C_{cell} ($F g^{-1}$) is the specific capacitance of the cell and ΔV (V) refers to the potential change within Δt (s). The average power density (P , $W g^{-1}$) was determined using the following relation:

$$P = E / \Delta t$$

Where E is the energy density and Δt is the discharge time.

2. Supplementary Figures and Tables

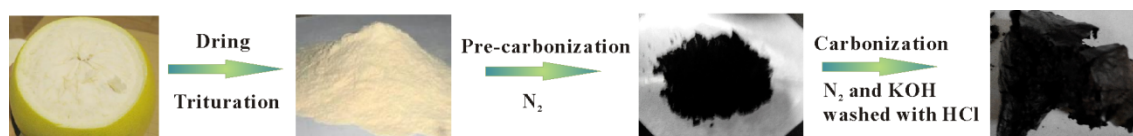


Fig. S1 Schematic diagram representing synthesis of HLPC

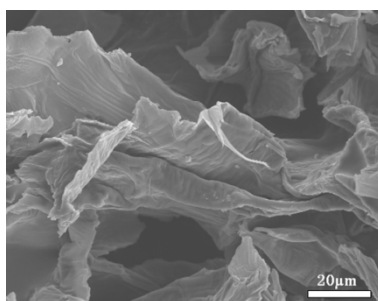


Fig. S2 SEM image of the primitive pomelo peel.

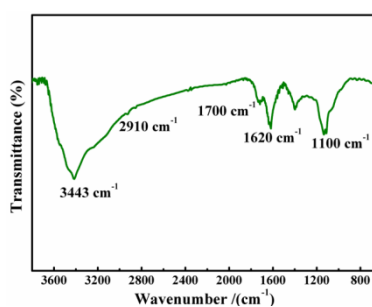


Fig. S3 the FT-IR spectrum of the HLPC

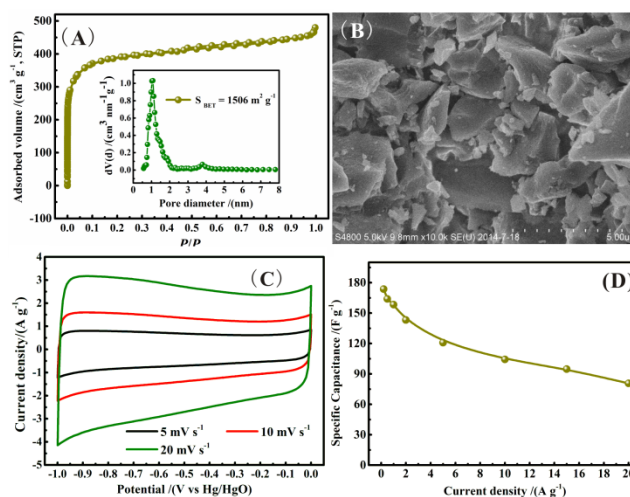


Fig. S4 (A) N_2 adsorption-desorption isotherms and the pore size distribution, (B) SEM image, (C) CV curves recorded at different scan rates, (D) variation of specific capacitance against current density of the commercial activated carbon (Kuraray YP-17D).

Table S1. Maximum capacitances of activated carbons from biomass precursors.

Precursor	$S_{BET}/(m^2 g^{-1})$	Electrolyte	$C/(F g^{-1})$	Reference
Fish scale	2237	6 M KOH	168	<i>J. Mater. Chem.</i> , 2010, 20 , 4773
Human hair	1306	6 M KOH	340	<i>Energy Environ. Sci.</i> , 2014, 7 , 379
Human hair	2100	6 M KOH	264	<i>Electrochim. Acta</i> , 2013, 107 , 397.
Tea-leaves	2841	6 M KOH	330	<i>Electrochim. Acta</i> , 2013, 87 , 401.
Cherry stones	1273	1M H_2SO_4	232	<i>Mater. Chem. Phys.</i> , 2009, 114 , 323.
Potato starch	2432	6 M KOH	335	<i>J. Phys. Chem. Solids</i> , 2009, 70 , 1256.
Starch	1510	6 M KOH	194	<i>Solid State Ionics</i> , 2008, 179 , 269.
Pig bone	2157	6 M KOH	185	<i>Carbon</i> , 2011, 49 , 838.
Seed shell	2509	30 wt% KOH	311	<i>Bioresour. Technol.</i> 2011, 102 , 1118
Sugar cane	1788	1 M H_2SO_4	300	<i>J. Power Sources</i> , 2010, 195 , 912
Cassava peel	1352	0.5 M H_2SO_4	153	<i>Bioresour. Technol.</i> , 2010, 101 , 3534
Pomelo peel	2725	6 M KOH	342	This work

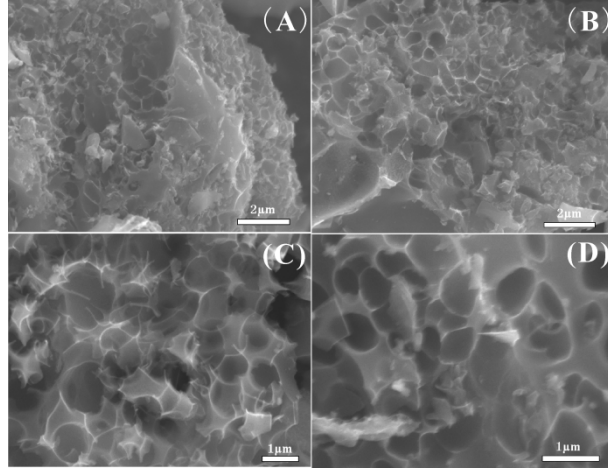


Fig. S5 SEM images of sample S1 (A), S2 (B), S3 (C), and S4 (D).

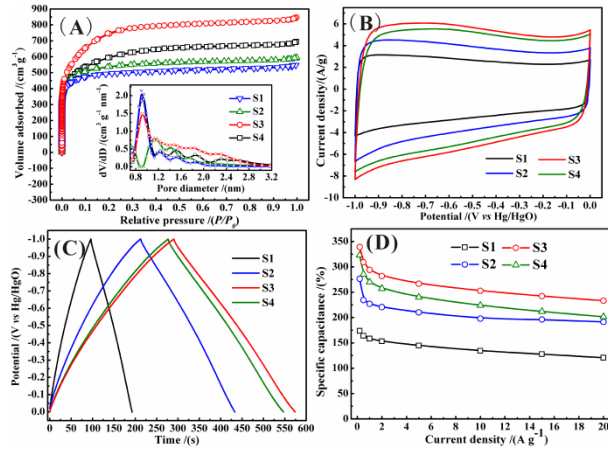


Fig. S6 (A) N_2 adsorption-desorption isotherms and the pore size distribution, (B) CV curves recorded at 20 mV s^{-1} , (C) GCD lines recorded at 1 A g^{-1} , and (D) variation of specific capacitance against current density of different samples.

Table S2 BET and pore parameters of different samples.

Sample Name	$S_{\text{BET}}^{\text{a}}$ /($\text{m}^2 \cdot \text{g}^{-1}$)	$S_{\text{meso}}^{\text{b}}$ /($\text{m}^2 \cdot \text{g}^{-1}$)	$S_{\text{micro}}^{\text{c}}$ /($\text{m}^2 \cdot \text{g}^{-1}$)	V_{t}^{d} /($\text{cm}^3 \cdot \text{g}^{-1}$)	$V_{\text{micro}}^{\text{e}}$ ($\text{cm}^3 \cdot \text{g}^{-1}$)	$V_{\text{meso}}^{\text{f}}$ /($\text{cm}^3 \cdot \text{g}^{-1}$)	$V_{\text{micro}} / V_{\text{total}}$
S1	1922	97	1825	0.819	0.731	0.088	0.892
S2	2014	89	1925	0.896	0.817	0.079	0.912
S3	2725	115	2610	1.277	1.164	0.113	0.912
S4	2163	80	2083	1.076	0.963	0.113	0.895

^a S_{BET} is calculated by the Brunauer–Emmett–Teller (BET) method. ^b S_{meso} represents the mesopore SSA. ^c S_{micro} refers to the total-pore volume that is determined using the DFT method. ^d V_{t} refers to the total-pore volume. ^e V_{micro} represents the micropore volume. ^f V_{meso} stands for the Barrett Mesopore volume obtained by subtracting V_{micro} from V_{t} .

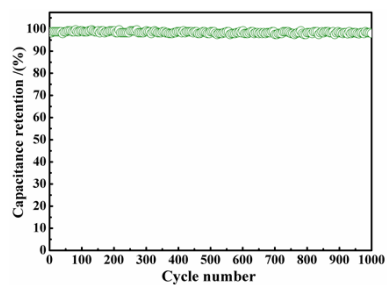


Fig. S7 Cycling performance of the symmetric SC device at 5 A g^{-1} in 6 M KOH

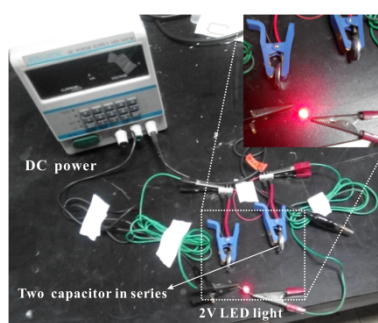


Fig. S8 Photograph of a red LED powered by the two SCs in series.

3. References

- (1) Tao, Y.; Xie, X.; Lv, W.; Tang, D.-M.; Kong, D.; Huang, Z.; Nishihara, H.; Ishii, T.; Li, B.; Golberg, D.; Kang, F.; Kyotani, T.; Yang, Q.-H., *Sci. Rep.* **2013**, *3*.
- (2) Yu, X.; Wang, J.-g.; Huang, Z.-H.; Shen, W.; Kang, F., *Electrochem. Commun.* **2013**, *36* (0), 66-70.